Int. J. Multiphase Flow. Vol. 4, pp. 53–64. Pergamon/Elsevier. 1978. Printed in Great Britain.

EXPERIMENTAL STUDY ON THE PRESSURE DROP AND THE ENTRY LENGTH OF THE GAS–SOLID SUSPENSION FLOW IN A CIRCULAR TUBE

A. SHIMIZU, R. ECHIGO and S. HASEGAWA
Department of Nuclear Engineering, Kyushu University, Fukuoka, Japan

and

M. HISHIDA
Japan Atomic Energy Research Institute, Ibaragi, Japan

(*Received* 23 *May* 1977; *received for publication* 10 *August* 1977)

Abstract—This paper presents an experimental study on the flow characteristics of a dilute gas–solid suspension medium in a circular tube, wherein the inlet entry length and the frictional pressure drop are measured systematically. In particular, the effects of particle size on the frictional pressure-drop are examined in some detail. The spherical copper particles, whose average diameter ranges from about 45 to 170 μm, are used for the dispersed medium and the ranges of gas Reynolds number and solid loading ratio are up to 50,000 and 5 respectively. The experimental results show that the entry lengths are feasible to be correlated briefly to the apparent Reynolds number of suspension flow and also that the reduction of the frictional pressure drop is observed at the lower loading ratio for the smallest size particles.

1. INTRODUCTION

In recent years, much attention has been paid toward gas–solid suspension flow as a heat-transfer medium that can be utilized under the condition of high temperature and high heat flux. The characteristic features of heat transfer for suspension flow would be summarized as follows (Depew & Kramer 1973).

1. Through the addition of the solid particles volumetric heat-capacity of the medium is increased in comparison with that of pure gas and that leads to an advantage of using it under the condition of high heat-flux.
2. In the vicinity of the wall, the solid particles generate disturbances in the laminar sublayer and reduce its effective thickness.
3. The radial motions of solid particles enhance the heat exchange between core region and near-wall region.
4. Presence of solid particles may reduce the turbulent motion of the gas and therefore reduce the convective heat-transfer.
5. Conversely, the wakes produced behind the particles may play a role of enhancing the turbulent motion of the fluid as the case may be.
6. In the region of high temperature where the thermal radiation plays an important role of heat transfer, the solid particles behave as absorbers or emitters of thermal radiation and increase the total heat-transfer rate (Echigo & Hasegawa 1972).

Concerning the pressure drop of gas–solid suspension flow in a duct, there have been numerous investigations especially associated with pneumatic conveying, and it is generally accepted that the additional pressure drop due to the addition of solid particles to the gas stream increases monotonously with solid loading ratio. Various kinds of works on this subject are reviewed systematically in the literature by Boothroyd (1971). In spite of the wide extent of these investigations, it appears to be difficult to obtain a universal relation between the pressure drop and the parameters of the flow, chiefly because there exist numerous factors that have influence upon the flow situation. It is worthwhile, therefore, to have a closer look at the parametric effect of each factor separately.

Boothroyd (1966), using considerably fine particles, carried out the experiments of suspension flow in a circular tube and found that the frictional pressure loss of suspension flow was less than that of single phase flow having the same velocity and attributed this phenomena to the fact that the solid particles suppress the turbulence of the flow (as mentioned above in 4th category). The reduction of convective heat-transfer at the same region of loading ratio is considered to be a proof of this reasoning. In his paper, he used the words "fine" and "coarse" particles and pointed out that such a reduction of frictional pressure loss is observed only for fine particles and the magnitude of this reduction strongly depends on the tube diameter for specified particles. However, the definite criteria were not shown explicitly for the particulate size or size distribution. Concerning this subject, Jotaki & Tomita (1973) gave the criteria for the particle size and friction velocity of the flow for occurrence of this reduction, based on the consideration toward the generation and dissipation processes of turbulent energy. The scarcity of experimental data, however, impedes more detailed discussion.

In this study, a lot of data on the pressure drop of suspension flow are obtained and plotted against the solid loading ratio. The solid particles used in this experiment were divided into several groups through sifting and the influence of particle diameter was examined in some detail.

Length of 25–70 tube diameters is considered to be necessary for the single-phase turbulent flow to be fully developed though the inlet conditions have influence to some extent. In many experimental studies of gas–solid suspension flow, each author checked on the development of the flow prior to his measurement. There seem to have been, however, few reports which paid direct attention to the entry length itself. For the problem of designing any kind of experimental or practical equipment for suspension flow, the entry length data are of great importance. Besides, as will be shown later, we observed great increases in entry length through adding the solid particles to the gas in all cases of our experiment. Consequently the situation that the entire part of heat-transfer tube lies in undeveloped region might possibly occur in case of practical purposes. From this point of view, many pressure taps were set along the test sections and the inlet entry length for suspension flow was examined experimentally.

2. EXPERIMENTAL EQUIPMENT

The gas–solid suspension flow used in this study is that of air and copper particles, the shapes of which are almost spherical. The copper particles were divided into several classes of their diameters through sifting. Figure 1 shows the particle size distributions. Three kinds of particle average diameters are listed in table 1 for all the powders shown in figure 1.

Figure 2 shows a schematic sketch of experimental apparatus. Two commercial vacuum cleaners are used as blowers and thus the pressure of the whole flowing line is vacuum from an atmospheric pressure. Merits of this adoption lie in the facts that the pulsating motion of the

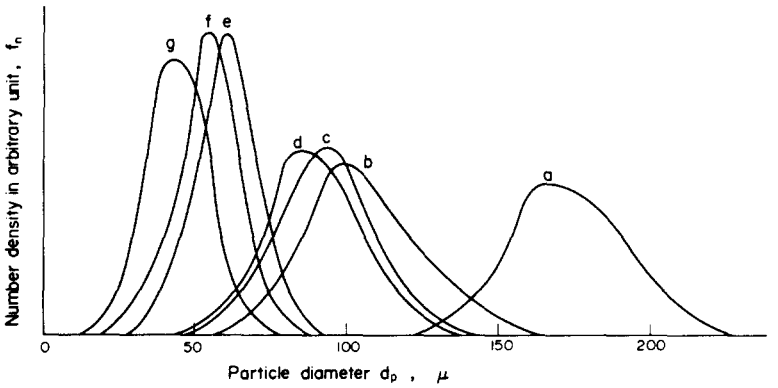

Figure 1. Particle size distribution for each powder.

Table 1. Particle average diameter

Powder	Particle average diameter, μ		
	d_p^1	d_p^s	d_p^v
a	172.1	173.6	173.7
b	103.2	107.2	107.5
c	96.8	98.4	98.8
d	89.9	91.8	92.2
e	59.0	60.0	60.9
f	52.8	53.9	54.9
g	44.7	45.8	46.7

$$d_p^1 = \int d_p f_n d(d_p) / \int f_n d(d_p)$$

$$d_p^s = \left(\int d_p^2 f_n d(d_p) / \int f_n d(d_p)\right)^{1/2}$$

$$d_p^v = \left(\int d_p^3 f_n d(d_p) / \int f_n d(d_p)\right)^{1/3}$$

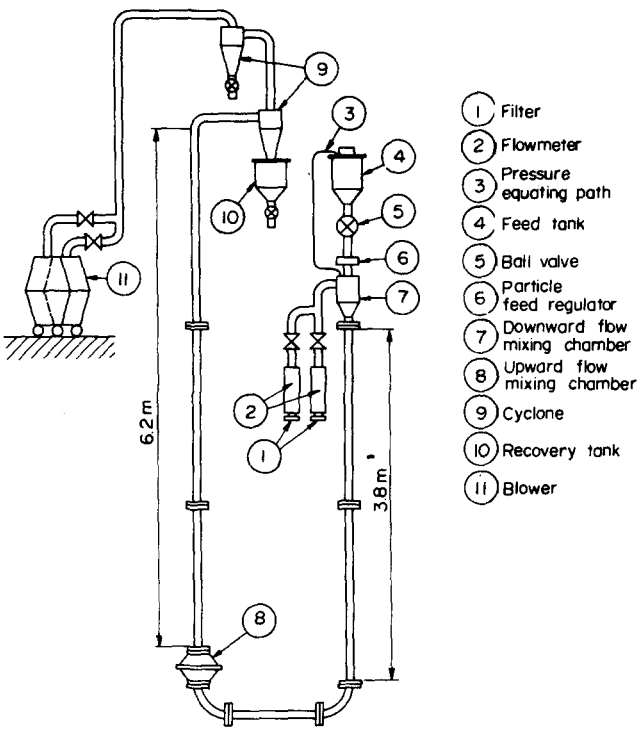

Figure 2. Experimental apparatus.

gas is smoothed and thus any surging tank is not necessary, and that we are free from the troubles of collecting the particles that have not been captured by cyclones. On the other hand, it is pointed out as a deficiency that the maximum gas flow rate is restricted to a certain value because the head along an entire line is 1 atm at most.

The copper particles, being weighed prior to each run of the experiment, are packed in the feed tank and dropped into the downward flow mixing chamber, the dropping rate of which is fixed at a certain value by a particle feed regulator. For the particle feed regulator, as shown in figure 3, a sliding plate of 5 mm thickness with several holes of 2 mm diameter is inserted into the flange section. A number of plates, each of which has different number of holes, are prepared and the solid feeding rate can be easily changed by replacing the sliding plate. As the pressure difference between atmosphere and the flow system is at the most 1 atm and the

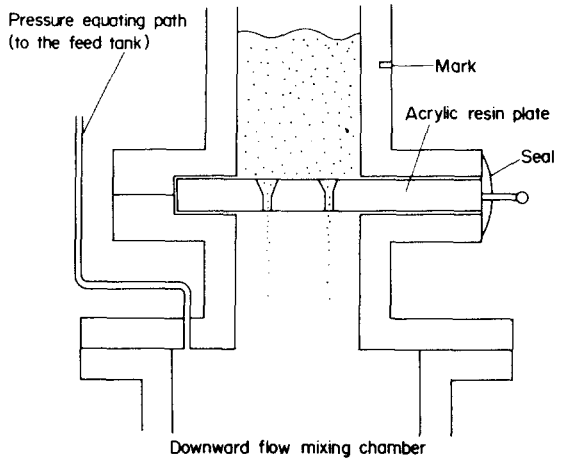

Figure 3. Particle feed regulator section.

system is of negative pressure, the air "leakage" into the system through the gaps between the sliding plate and the flange is sealed by padding the "oil clay" as also shown in the figure. A mark was put on the acrylic resin pipe at the point of 5 cm above the flange, and the weight of the powder at the time when the powder's upper surface coincided with that mark was measured in advance. Total amount of the powder used for measurement is acquired by subtracting the value mentioned above from the initially packed weight of the powder. In order to obtain the solid feed rate, we divide the total amount of the powder by the time interval between opening the ball valve and the moment when the powder's upper surface comes down to the mark. The reason why such a procedure is employed to obtain the solid feed rate lies in the fact that the solid falling rate from the holes of the sliding plate is not constant with time just before the feed regulator section is emptied. Furthermore, a pressure equating path is set up, connecting the mixing chamber with the upper space of the powder in the feed tank. Through these contrivances, the solid feed rate can be kept constant. The constancy was verified through the other simpler equipment beforehand and found to be satisfactory.

Fluctuation of solid feed rate for a specified plate is so small even when the air flow rate in the mixing chamber is changed that the solid loading ratio is easily fixed at any desired value.

Air is introduced into the mixing chamber by way of filter and flowmeter. The test sections of the downcomer and of the riser are both made of acrylic resin pipes with 28 mm inner diameter connected by flanges, and the pipes are transparent for the visual observation. Another mixing chamber is installed prior to the riser tube so as to measure the entry length for upward flow of gas–solid suspension.

The variations of static pressure along the flowing line are measured with pressure taps of 1 mm diameter which are drilled at 200 mm intervals along the tube. Two pairs of pressure taps are selected at the lowest portion for the downward flow and the highest for the upward flow, the intervals of which are 1.0 m and 1.6 m respectively, and they are connected to a Göttingen manometer in order to obtain accurate measurement of the pressure drop. Leaving the riser test tube, the suspension flow enters the first cyclone and the larger part of the particles is separated from the gas stream and stored in the recovery tank. The amount of the particles that has not been recovered is captured by the second cyclone connected in series with the first one.

3. EXPERIMENTAL PROCEDURE AND DATA ANALYSIS

Prior to the measurements of the suspension flow, we obtained the data of the pressure drop for single phase flow and compared them with the Blasius' relation for smooth circular tube.

$$\lambda_0 = 0.3164\, Re^{-1/4}. \qquad [1]$$

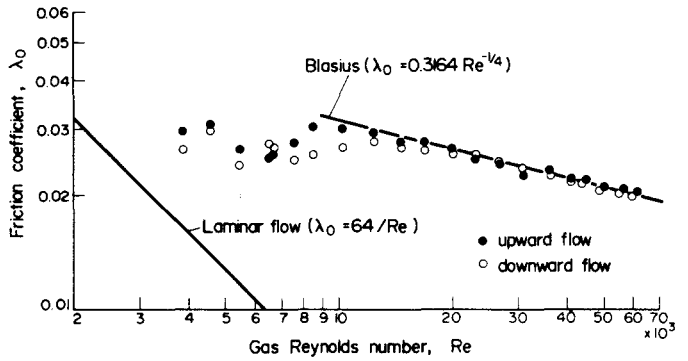

Figure 4. Friction coefficient without suspension.

The results are shown in figure 4 and the agreement is found to be satisfactory at Reynolds number above 10,000. At Reynolds number less than 10,000, the scatter of the data is observed chiefly because the pressure difference between the two points of measurement is too small to be accurately measured with the water manometer. Subsequently, the pressure drops for suspension flows were measured for all of the sliding plates, the Reynolds number being manipulated to a certain value by adjusting the gas flow rate. Through these measurements the solid falling rate for each sliding plate was estimated and the result was used in measurements for prescribed loading ratio. The same procedure was repeated for all the powders of figure 1.

Let ΔP_m be the measured total pressure difference along the flowing line of length l. This may be written in the following form,

$$\Delta P_m = \Delta P_{as} + \Delta P_{ag} + \Delta P_{ps} + \Delta P_t \qquad [2]$$

where four terms in the R.H.S. represent the pressure drop due to the acceleration of the solid particles, due to the acceleration of the gas, due to the gravitational force acting on the solid particles, and due to friction, respectively. The sign before ΔP_{ps} must be changed in case of the downward flow. The gravitational head of the gas is not necessary to be considered here because the pressure difference between two points is directly measured with a single manometer filled with the same gas in the flowing line.

ΔP_{as} and ΔP_{ag} are both neglected in the present analysis on the assumption that all the suspension flows of the present experiment are fully developed at the position of the pressure drop measurement. The validity of this assumption will be discussed later.

In order to estimate the gravitational pressure difference which is necessary to sustain the column of the dispersed solid particles, Boothroyd (1966) neglected the relative velocity between solid particles and gas, and this is justified in view of the considerably fine powders used in his measurement. The calculation based on the well-known drag curve of a single sphere gives the free falling terminal velocity of about 3.2 m/sec for the copper particle of 172 μm diameter, while the lowest gas velocity of suspension flow of the present study is about 5 m/sec. Accordingly we are not allowed to neglect the relative velocity in evaluating the gravity effect in our case.

Yang (1973) presented the corrected form of the relative velocity between two materials taking into account the presence of the tube wall and/or the mutual interactions of the dispersed particles. His corrected relative velocity is expressed as

$$U_{pt} = \sqrt{\left[\left(1 + \lambda_p \frac{U_s^2}{2g_c D}\right) \frac{4(\rho_s - \rho_g) d_p g_c}{3\rho_g C_{DS}} \epsilon^{4.7}\right]} \qquad [3]$$

where U_s, D, C_{DS}, and ϵ denote the average solid velocity, the tube diameter, the drag coefficient

of a single particle, and the voidage of the suspension within the tube, respectively. Equation [3] is reported to be able to correlate the existing particle velocity data within 20%. Equation [3] includes the particle drag coefficient λ_p defined as,

$$\Delta P_t = \Delta P_{tg} + \Delta P_{ts} = l\lambda_g \rho_g U_g^2/2D + l\lambda_p \rho_{dp} U_s^2/2D \qquad [4]$$

where ΔP_{tg} and ΔP_{ts} are frictional pressure drop due to gas and that due to solid, respectively, and ρ_{dp} denotes dispersed density of the suspension, $\rho_{dp} = \epsilon\rho_g + (1-\epsilon)\rho_s$. The friction coefficient without suspension is usually used as λ_g, because measured frictional pressure drop can not be divided into two parts on the reasonable ground. The adaption of [4] is, therefore, accompanied with the underlying concept that the addition of the solid particles into the gas stream always enhances the frictional pressure drop, and this is always the case with relatively coarse particles and higher loading ratio. If this analysis is applied to the Boothroyd's data, however, which show the reduction of frictional pressure drop, the negative value of λ_p would be obtained so far as the friction coefficient for gaseous phase is assumed to be unchanged, and that is inconsistent with the concept of λ_p.

In the present study, this reduction of frictional pressure drop is observed for the smallest particles of the figure 1 at the loading ratio region less than 0.6. Two ways of the data analysis were tried, one based on the [3] and the other based on the assumption that the relative velocity was equal to the terminal velocity and the difference between the two procedures was found to be not substantial compared with the experimental uncertainty. Hence the experimental results shown later are based on the second procedure. Namely, the relative velocity U_{pt} is obtained through the following equation.

$$U_{pt} = \sqrt{\left(\frac{4g_c d_p(\rho_s - \rho_g)}{3\rho_g C_{DS}}\right)}. \qquad [5]$$

As the particle drag coefficient C_{DS} is a function of the particle Reynolds number, $Re_p = U_{pt}d_p/\nu$, the iterative calculation is necessary. Solid loading ratio Γ is defined as a ratio of mass flow rate of solid to that of gas

$$\Gamma = \frac{W_S}{W_g} = \frac{U_s\rho_s(1-\epsilon)}{U_g\rho_g\epsilon}. \qquad [6]$$

Hence

$$\Delta P_{\rho s} = lg_c\rho_s(1-\epsilon) = lg_c\rho_s \frac{\Gamma U_g\rho_g}{\Gamma U_g\rho_g + U_s\rho_s}, \qquad [7\text{-a}]$$

$$U_S = U_g \pm U_{pt}, \qquad [7\text{-b}]$$

$$\Delta P_t = \Delta P_m \pm \Delta P_{\rho s}. \qquad [7\text{-c}]$$

(+; downward, −; upward)

No attempt was made in this study to separate ΔP_t into two parts as in [4] in connection with the above discussion.

4. RESULTS AND DISCUSSION

4.1 *Entry length*

Figures 5 and 6 show some typical results of measurements of static pressure along the test tubes of upward and downward flows, respectively. In both figures whole data are moved parallel in the vertical direction so that all the values of first pressure tap may coincide. The

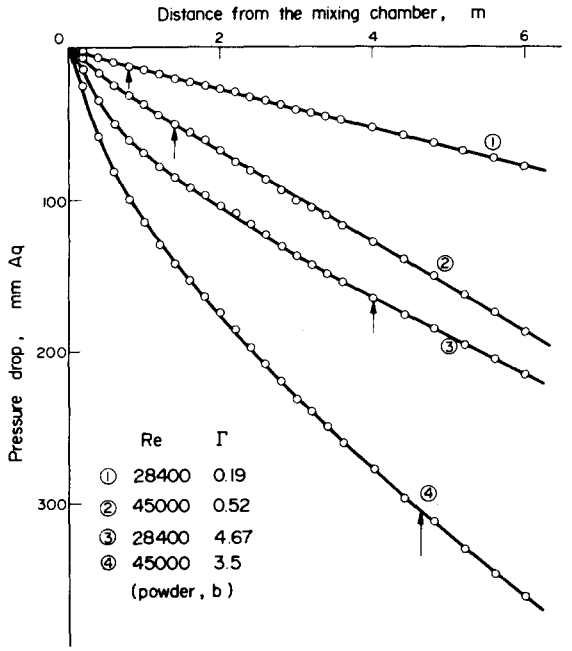

Figure 5. Pressure in upward flow with respect to that at the inlet position.

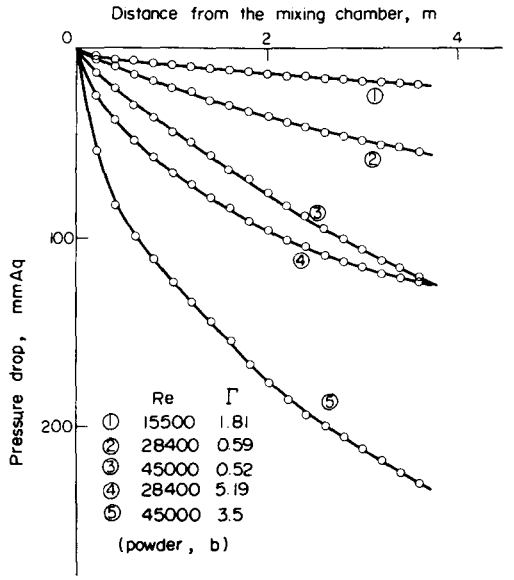

Figure 6. Pressure in downward flow with respect to that at the inlet position.

arrows depicted in the figure 5 indicate the locations where each flow is considered to become fully developed, and the distance from the mixing chamber up to this point is tentatively regarded as an entry length. This procedure of evaluating the entry length seemingly yields an uncertainty because of the manipulative errors. It is, however, of great importance from the practical point of view to know the relevance of the entry length to the flow conditions of the gaseous suspensions. Thus, it would be feasible to get the general trend of the entry length, provided that a number of experimental data are obtained.

Unfortunately, examination of the figure 6 reveals that the downcomer tube was too short to realize the fully developed downward suspension flow even at the lowest section of it. Therefore ΔP_f for the downward flow would not be estimated exactly unless the accurate radial

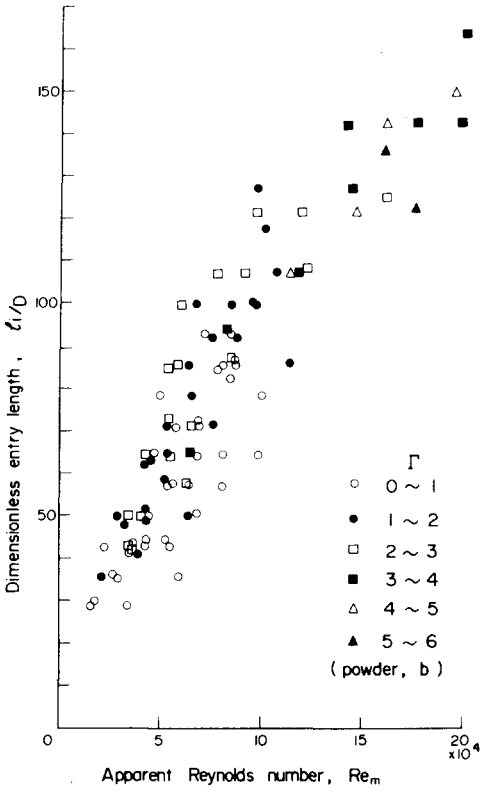

Figure 7. Dimensionless entry length for upward flow.

velocity profiles for both phases at the two points were known. In contrast with the downward flow, all the upward flows are considered to be fully developed at the end of the riser.

The entry lengths in dimensionless form, l_t/D, for upward flow are plotted in figure 7 as a function of apparent suspension flow Reynolds number defined as

$$Re_m = \frac{(\epsilon\rho_g U_g + (1-\epsilon)\rho_s U_s)D}{\mu} = \left(1 + \frac{(1-\epsilon)\rho_s U_s}{\epsilon\rho_g U_g}\right)\frac{\epsilon\rho_g U_g D}{\mu} \approx (1+\Gamma)Re \qquad [8]$$

(Even the highest volume fraction of the particles of the present study was less than 0.001).

It should be noted from the figure that the entry length for upward flow is a monotonously increasing function of Re_m and that the slope of increasing becomes gradually smaller as Re_m increases. The arrangement of the entry length by means of Re_m seems to be acceptable for a provisional correlation,

4.2 *Frictional pressure drop*

Figure 8 shows the total and frictional pressure drops for both upward and downward flows divided by those of the single phase flow having the same gas velocity. The difference between $\Delta P_m/\Delta P_0$ and $\Delta P_t/\Delta P_0$ corresponds to the correction of the gravity effect discussed in the preceding section. According to the results of the entry length measurement, we might be allowed to suppose that the entry length for downward flow would become also shorter for lower Reynolds number if the flowing conditions including the velocity profile and the turbulence structure are not substantially different from those of the upward flow. Hence the fact that ΔP_t for both upward and downward flows are of almost same value in the lower Reynolds number case [figure 8—(1)] suggests that the method of evaluating the gravitational contribution of the suspended particles is reasonable. In figure 8—(2), which shows the higher Reynolds number case, ΔP_t of the downward flow is considerably greater than that of the

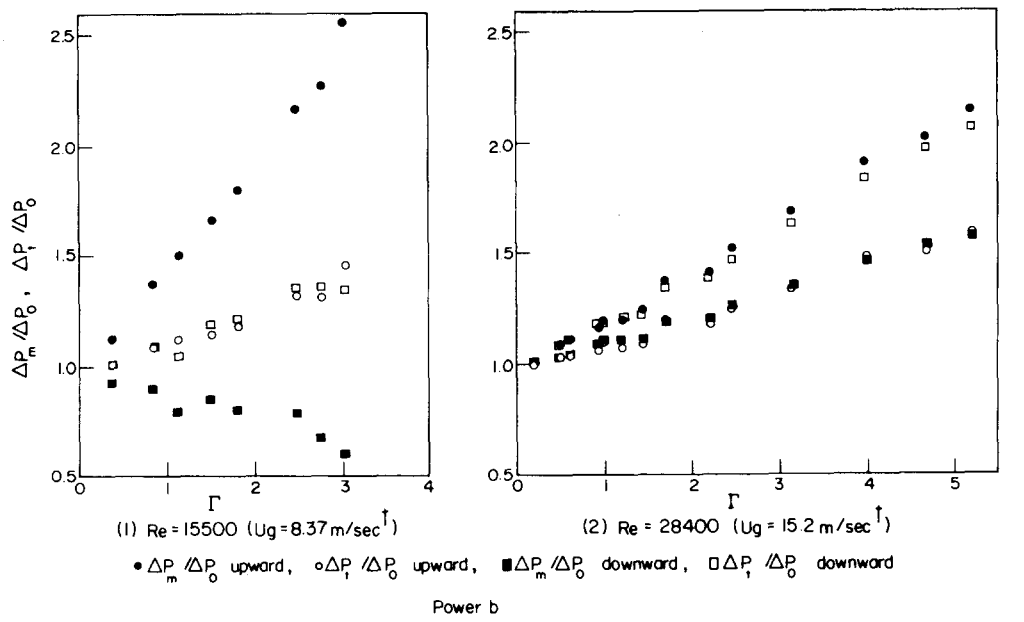

Figure 8. Total and frictional pressure drop both divided by those without suspension.

upward flow, and this is ascribed to the gradual extension of the entrance region to the pressure measurement part (see figure 6), hence ΔP_t for the downward stream becomes less trustworthy.

Figure 9 shows the frictional pressure drop ratio of the upward flow for the same powder as shown figure 8, the Reynolds numbers of which, however, are different from those of the figure 8. Other author's results are also shown in the figure for comparison. Figures 8 and 9 reveal that the additional frictional pressure drop due to the presence of the solid particles follows the linear relation with the solid loading ratio for the specified powder. Leung & Wiles (1976) recently reviewed various works on this subject and proposed the following equation for the particle friction coefficient,

$$\lambda_s = 0.2 U_s^{-1} (U_s, \text{in m/sec}) \qquad [9\text{–a}]$$

where

$$\Delta P_t = \Delta P_{tg} + \Delta P_{ts} = l\lambda_g \rho_g U_g^2/2D + l\lambda_s(1-\epsilon)\rho_s U_s^2/2D. \qquad [9\text{–b}]$$

Assuming that the frictional pressure drop due to gas is equal to that without suspension, we obtain,

$$\frac{\Delta P_t}{\Delta P_0} = 1 + \frac{\lambda_s(1-\epsilon)\rho_s U_s^2}{\lambda_g \rho_g U_g^2} = 1 + \epsilon \frac{\lambda_s U_s}{\lambda_s U_g}\Gamma \approx 1 + \frac{0.2}{0.3164 Re^{-1/4} U_g}\Gamma = 1 + R\Gamma$$

$$(U_g, \text{in m/sec}) \qquad [10]$$

The value of Reynolds number 45000 ($U_g \approx 24.3$ m/sec) gives the slope $R = 0.379$ and this is also shown in the figure. It is noticed that the data of the current study are considerably lower than the equation of Leung & Wiles (1976) and that they are rather close to the data of the experiments with finer powder.

Concerning the effect of the Reynolds number on the frictional pressure drop ratio, any decisive conclusion would not be derived from figure 9 because of the scatter of the data. Nevertheless, increase of the Reynolds number seems to bring about the slight increase in the slope R for the parameter region shown in the figure.

†Gas velocity U_g is slightly scattering for the specified Reynolds number, because it was adjusted to give the same value of the Reynolds number at the test section irrelevant to pressure and temperature.

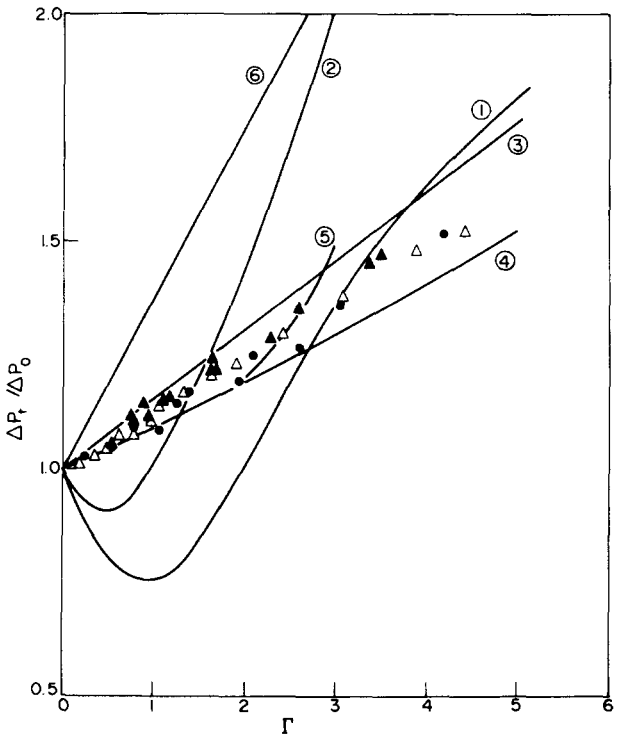

	Tube diam.	Re	Particle	Particle size	Gas	
•	28 mm	21700	copper	103 μ	air	present work
△	28	36000	copper	103	air	present work
▲	28	45000	copper	103	air	present work
①	50.8	53000	zinc	10	air	cited from the Boothroyd's paper (1966)
②	76.2	53000	zinc	10	air	cited from the Boothroyd's paper (1966)
③	12.7	8000	graphite	5	argon	cited from the Boothroyd's paper (1966)
④	12.7	17000	graphite	5	nitrogen	cited from the Boothroyd's paper (1966)
⑤	18.0	27400	glass	36	air	cited from the Boothroyd's paper (1966)
⑥	—	45000	——	——	——	Leung Eq. [10]

Figure 9. Frictional pressure drop ratio.

4.3 *Effect of the particle diameter*

Four powders of figure 1, particle size distributions of which are clearly distinguishable from each other, are chosen and the frictional pressure drops of them are shown in figure 10. The logarithmic abscissa is used in order to lay emphasis on the lower loading ratio region. Results of the other powders, the particle size distributions of which are not so distinguishable from each other as in case of the above four powders, i.e. of the powder (b) (d) for example, were also indistinguishable in view of the experimental uncertainty. Hence they are omitted from the figure for the sake of clarity. For the largest particles, i.e. powder (a), the frictional pressure drop ratio is always greater than 1.0 and is an increasing function of the solid loading. On the contrary it is noticed that the reduction of the frictional pressure drop is observed at the region of solid loading less than about 0.6 for the smallest particles. In figures 7–9 of Boothroyd's paper even the measured pressure drops are found to be less than those without suspension. In the present study, such a reduction of the total pressure drop was not observed for all the values of parameters examined.

Jotaki & Tomita (1973) proposed several conditions for occurrence of the reduction of frictional pressure drop. Essential points of their conditions are that the solid particle must be large enough not to follow the fluctuating motion of the gas, and that at the same time it must be so small that the particle Reynolds number produced by the fluctuating component of the gas velocity around the particle, lies within Stokes' region and so no additional turbulent motion is generated by the presence of the particle. The last condition is expressed by the friction

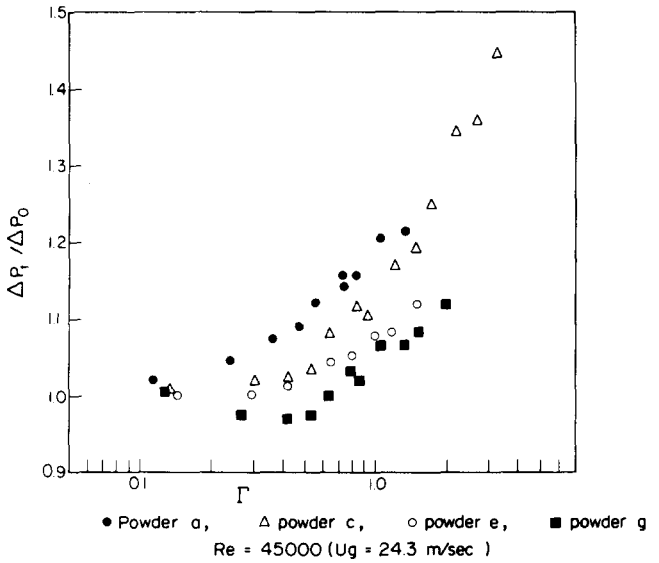

Figure 10. Effect of the particle size on the frictional pressure drop ratio.

velocity u^*,

$$\frac{2d_p u^*}{\nu} < 1. \qquad [11]$$

Experimental point that gives the lowest frictional preseure drop ratio in figure 10 (d_p = 44.7μ, Γ=0.41, Re = 45000) gives the friction velocity u^* = 1.43 m/sec [$u^* = \sqrt{(\tau_w/\rho_f)} = \sqrt{(D\Delta P_f/\rho_f 4l)}$]. These values do not satisfy [11]. Exactly speaking, however, their conditions are considered to be unnecessary but sufficient conditions and could be loosened so far as the presence of the solid particles leads to the net consumption of the turbulent energy. Qualitatively, the effect of the particle diameter shown in the figure 10 is considered to be in accordance with the interpretation of Jotaki & Tomita (1973).

5. SUMMARY

The experimental study of gas–solid suspension flow is carried out and the results are summarized in the following.

1. The inlet entry length of the upward flow can be well correlated to the apparent suspension flow Reynolds number Re_m and is found to be an increasing function of Re_m.

2. The frictional pressure drop due to the addition of the solid particles follows the linear relation with solid loading ratio for the coarser particles, although the magnitude of them is rather smaller among the works reported so far.

3. The reduction of the frictional pressure drop is observed at the lower loading ratio region for the smallest powder and the decrease of the particle diameter brings about the decrease of the frictional pressure drop ratio.

Acknowledgements—Authors gratefully acknowledge the cooperation of the experiment to former students, Messrs. S. Matsuo, M. Fujisaki, and H. Yoshiki. This work was partially supported by the research fund (Grant No. 111004) of the Ministry of Education of Japan.

REFERENCES

BOOTHROYD, R. G. 1966 Pressure drop in duct flow of gaseous suspensions of fine particles. *Trans. Instn Chem. Engrs* **44**, T306–T313.

BOOTHROYD, R. G. 1971 *Flowing Gas–Solid Suspensions*. Chapman & Hall, New York.

DEPEW, C. A. & KRAMER, T. J. 1973 Heat transfer to flowing gas–solid mixtures. *Adv. Heat Transf.* **9**, 113–180.

ECHIGO, R. & HASEGAWA, S, 1972 Radiative heat transfer by flowing multiphase medium *Int. J. Heat Mass Transfer* **15**, 2519–2534.

JOTAKI, T. & TOMITA, Y. 1973 Turbulent friction drag of a dusty gas. *Bull. J.S.M.E.* **16**, 93–99.

LEUNG, L. S. & WILES, R. J. 1976 A quantitative design procedure for vertical pneumatic conveying systems. *I/EC Process Des. Dev.* **15**, 552–557.

YANG, W. C. 1973 Estimating the solid particle velocity in vertical pneumatic conveying lines. *I/EC Fundamentals* **12**, 349–352.